Cerebral Cortex February 2010;20:304–314
doi:10.1093/cercor/bhp100
Advance Access publication May 29, 2009

Tis21 Expression Marks Not Only Populations of Neurogenic Precursor Cells but Also New Postmitotic Neurons in Adult Hippocampal Neurogenesis

Alessio Attardo[1,4], Klaus Fabel[2,3], Julia Krebs[2,3], Wulf Haubensak[5], Wieland B. Huttner[1] and Gerd Kempermann[2]

[1]Max Planck Institute of Molecular Cell Biology and Genetics, 01307 Dresden, Germany, [2]Center for Regenerative Therapies Dresden, Genomics of Regeneration, 01307 Dresden, Germany and [3]Department of Psychiatry and Psychotherapy, Technische Universität Dresden, 01307 Dresden, Germany

[4]Current address: Department of Biological Science, Stanford University, Stanford, California 94305, USA
[5]Current address: California Institute of Technology, Pasadena, California 91125, USA

Alessio Attardo, Klaus Fabel, Wieland B. Hunter and Gerd Kempermann have contributed equally to this study.

During embryonic cortical development, expression of Tis21 is associated with cell cycle lengthening and neurogenic divisions of progenitor cells. We here investigated if the expression pattern of Tis21 also correlates with the generation of new neurons in the adult hippocampus. We used *Tis21* knock-in mice expressing green fluorescent protein (GFP) and studied *Tis21*-GFP expression together with markers of adult hippocampal neurogenesis in newly generated cells. We found that *Tis21*-GFP 1) was absent from the radial glia–like putative stem cells (type-1 cells), 2) first appeared in transient amplifying progenitor cells (type-2 and 3 cells), 3) did not colocalize with markers of early postmitotic maturation stage, 4) was expressed again in maturing neurons, and 5) finally decreased in mature granule cells. Our data show that, in the course of adult neurogenesis, Tis21 is expressed in a phase additional to the one of the embryonic neurogenesis. This additional phase of expression might be associated with a new and different function of Tis21 than during embryonic brain development, where no Tis21 is expressed in mature neurons. We hypothesize that this function is related to the final functional integration of the newborn neurons. Tis21 can thus serve as new marker for key stages of adult neurogenesis.

Keywords: dentate gyrus, mouse, neural stem cell, precursor cell

Introduction

Adult neurogenesis is not just the continuation of embryonic neurogenesis in 2 distinct neurogenic sites of the adult brain. During embryonic neurogenesis, the task is to generate a very high number of new neurons in an efficient and coordinated way, whereas adult neurogenesis has to deliver a small number of newborn neurons that need to be able to wire into an existing neuronal network. We here asked whether embryonic and adult neurogenesis follow a similar program in their progression from an uncommitted stem cell–like precursor to a fully integrated functional neuron. For this purpose, we studied the expression of Tis21. *Tis21* is an antiproliferative gene involved in the control of cell cycle progression, specifically in the G1 to S transition (Rouault et al. 1996; Guardavaccaro et al. 2000), and is specifically expressed in neurogenic precursor cells but not in postmitotic neurons during embryonic neurogenesis (Iacopetti et al. 1994, 1999; Haubensak et al. 2004). To investigate neuronal commitment of progenitor cells in the adult hippocampus, we used a knock-in mouse line expressing nuclear green fluorescent protein (GFP) under the control of the *Tis21* promoter (Haubensak et al. 2004). During embryonic neurogenesis, Tis21-expressing progenitors in the cortex divide asymmetrically and symmetrically to generate neurons (Haubensak et al. 2004; Attardo et al. 2008). Moreover, Tis21 expression has been associated with the switch from proliferation to neurogenesis and lengthening of the cell cycle during embryonic neurogenesis (Canzoniere et al. 2004; Calegari et al. 2005) and precedes neuronal differentiation during hippocamapal adult neurogenesis (Farioli-Vecchioli et al. 2008). Adult hippocampal neurons originate from a radial glia–like precursor cell (type-1) in the subgranular zone (SGZ) of the dentate gyrus (DG) through a number of intermediate cell types (type-2 and 3). After an early postmitotic maturation stage, associated with dendrite and axon elongation and selective survival, the newborn granule cells fully integrate into the DG circuitry (van Praag et al. 2002; Kempermann and Jessberger 2003; Song et al. 2005). Type-2 cell stage marks the transition between cells with a glial phenotype (type-2a cells) and cells with early features of the neuronal lineage (type-2b cells). Characterization of type-2 cells, using a panel of different markers (Sox2, Blbp, doublecortin [Dcx], and NeuroD1), suggested that whereas type-2a cells feature, to some degree, properties of radial glia–like cells (Blbp and Sox2 immunoreactivity), type-2b cells are committed to the neuronal lineage. Type-3 cells generate progeny that exits from the cell cycle and begins the terminal postmitotic differentiation of granule cells (Kempermann et al. 2004; Steiner et al. 2006).

Given the selective expression of Tis21 during embryonic neurogenesis, we hypothesized that Tis21 might allow the identification of neurogenic progenitors in the adult DG. If Tis21 was associated with neurogenic precursor cell divisions as it is the case in the fetal brain, we would expect Tis21 expression in type-2 cells and/or in type-3 cells.

In this study, we analyzed Tis21 expression patterns in the hippocampal DG and other brain areas of postnatal and adult mouse brain using the *Tis21*-GFP knock-in mouse line.

Materials and Methods

Mice Handling and Tissue Preparation

Tis21-GFP heterozygous mice were kept in standard housing conditions; all experiments were carried out according to local and federal regulations regarding research with animals. *Tis21*-GFP heterozygous mice, either untreated or injected with bromodeoxyuridine (BrdU; 50 mg/kg in 0.9% saline; Sigma, Munich, Germany) twice with a 3-h interval between injections, were deeply anesthetized with a mixture of ketamine/xylazine (ketamine 50 mg/kg and xylazine 10 mg/kg in phosphate-buffered saline [PBS]) and perfused with 0.9% NaCl and 4%

cold paraformaldehyde (PFA) in phosphate buffer. Brains were removed, postfixed overnight in 4% PFA in phosphate buffer, equilibrated in 30% sucrose for an additional 24 h at 4 °C, and then sectioned in the coronal plane using either a cryostat or a freezing microtome. Ten-micron cryosections were collected on RNAase-free coated slides for in situ hybridization. Forty-micron sections were collected and stored at –20 °C in fluid cryoprotectant containing 25% ethylene glycol, 25% glycerine, and 0.05 M phosphate buffer until use for immunohistochemistry.

In Situ Hybridization

Nonradioactive in situ hybridization using digoxigenin-labeled (DIG-RNA labeling kit, Roche, Mannheim, Germany) cRNA antisense and sense probes corresponding to the full open reading frame of the enhanced GFP gene (Clontech, Heidelberg, Germany) was carried out on 10-μm cryosections of perfused brains according to standard methods. The sections were equilibrated for 15 min in PBS and then prehybridized for 1 h at 65 °C in the hybridization mix (50% formamide, 10% dextran sulfate, 1× standard saline citrate (SSC), 1× Denhardt's solution, and salmon sperm DNA 40 μg/mL). The probes were denatured for 10 min at 80 °C and added to the hybridization mix (600 ng/mL). The hybridization reaction was carried out at 65 °C overnight. After incubation, the sections underwent the following washes 1) twice for 40 min in 50% formamide, 0.1% Tween 20, and 2× SSC at 65 °C, 2) twice for 5 min in 2× SSC at room temperature (RT), 3) twice for 5 min in TNT (0.1 M Tris–HCl, pH 7.5, 0.15 M NaCl, and 0.1% Tween 20) at RT, and 4) once for 20 min in TNT at RT. Then the sections were equilibrated for 30 min in TNT supplemented with 10% fetal calf serum at RT. The sections were incubated overnight at 4 °C with alkaline phosphatase–coupled anti-DIG antibody (Boehringer Mannheim, Mannheim, Germany) diluted 1:2000 in TNT supplemented with 10% fetal calf serum. After incubation, the sections were washed twice for 5 min in TNT at RT and then equilibrated for 30 min in B1 (0.1 M Tris–HCl, pH 9.5, 0.1 M NaCl, 50 mM $MgCl_2$, and 0.1% Tween 20). Color development was performed at RT (12–24 h) in B1 containing 5-bromo-4-chloro-3′-indolyphosphate p-toluidine salt (BCIP) and nitro-blue tetrazolium chloride (NBT) (both Boehringer Mannheim). Staining was stopped by a 10-min wash in PBS.

Immunohistochemistry

Free-floating tissue sections were blocked for 1 h in a solution of Tris-buffered saline (TBS) containing 10% preimmune donkey serum (DS) (Jackson ImmunoResearch, Westgrove, PA) and 0.3% Triton X-100 and then incubated with primary antibodies in TBS containing 3% DS and 0.3% Triton (TBS+) at 4 °C overnight: anti-phospho-histone 3 (PH3), rabbit, 1:400 (Upstate Signaling/Millipore, Schwalbach, Germany); anti-Ki67, rabbit, 1:500 (Novocastra, Newcastle, UK); anti-glial fibrillary acidic protein (GFAP), guinea pig, 1:800 (Advanced ImmunoChemicals, Long Beach, CA); anti-GFAP, rabbit, 1:800 (Dako Cytomation, Vienna, Austria); anti-BLBP, rabbit, 1: 500 (Abcam, Cambridge, UK); anti-nestin, mouse, 1:400 (US Biological, Swampscott, MA); anti-S100β, rabbit, 1:1000 (Swant, Bellinzona, Switzerland); anti-Sox2, rabbit, 1:250 (Chemicon, Temecula, CA); anti-Dcx, goat, 1:250; anti-NeuroD1, goat, 1:200 (both Santa Cruz, Santa Cruz, CA); anti-calretinin (CR), goat, rabbit, 1:400 (both Swant); anti-NeuN, mouse, 1:150 (Chemicon); and anti-calbindin (CB) (clone DK28), mouse, 1:400 (Swant). Afterward, sections were washed with TBS and incubated with secondary fluorochrome-conjugated antibodies (fluorescein isothiocyanate [FITC]-conjugated donkey anti-mouse, 1:500; FITC-conjugated donkey anti-rabbit, 1:500; Cy3-conjugated donkey anti-goat, 1:500; Cy3-conjugated donkey anti-guinea pig, 1:500; and Cy5-conjugated donkey anti-rat, 1:500; all from Jackson ImmunoResearch) in TBS+ for 4 h at RT. Sections were washed in TBS, nuclei were stained using Hoechst 33342 (Sigma), washed again in TBS, and mounted on uncoated glass slides using polyvinyl alcohol with 1,4-Diazabicyclo[2.2.2]octane (PVA-DABCO; Sigma).

For BrdU detection, immunostained tissue sections were postfixed for 15 min with 4% PFA in phosphate buffer, washed in TBS, incubated in 2 M HCl for 30 min at 37 °C, and neutralized with several washes with TBS. Tissue sections were blocked and incubated with a primary antibody anti-BrdU, rat, 1:500 (Accurate Chemical, Westbury, NY) in TBS+ at 4 °C overnight, washed with TBS, and incubated with secondary antibodies (Cy5-conjugated donkey anti-rat, 1:500) in TBS+ for 4 h at RT. Floating tissue sections were further treated as described above.

Cell Counts

Single focal plane images of fluorescence-labeled 40-μm *Tis21*-GFP heterozygous mice brain slices including the entire DG were acquired using a Zeiss 510 confocal laser-scanning microscope. Appropriate gain and black-level settings were determined on control tissues stained with secondary antibodies alone; upper and lower thresholds were set using the range indicator function to minimize oversaturation in positive cells. Three or more stacks of images were acquired per single tissue section, representative of the rostral, mid, and caudal hippocampus. Analysis of the images was carried out offline using Zeiss LSM510 software. To calculate the proportions of each cell phenotype as well as the phenotypes of the BrdU positive, cells were scored within the dentate granule cell layer (GCL) including 20 μm of the adjacent hilar margin SGZ in 2 or 3 different focal planes.

Stereology

Stereology was performed to determine the total number of cells in the DG GCL and SGZ (Nissl staining) and of BrdU-positive cells (diaminobenzidene histochemistry). Stained nuclei and BrdU-positive cells were scored in every sixth 40-μm section spanning the right DG in its complete rostrocaudal extent. All counts were limited to the hippocampal GCL and SGZ. The total numbers of Nissl-positive cells were determined with the optical fractionator method using the semi-automated stereology system StereoInvestigator® (MicroBrightfield, Magdeburg, Germany) with a Hitachi HV-C20A video camera attached to a Leica DM 5500 microscope. The DG was outlined using the 20× objective, and the actual section thickness was measured. A 63× oil immersion objective (1.4 NA) and a counting frame of 20 × 20 μm was used for counting Nissl-positive cells in a grid size of 100 × 100 μm. A 40× air objective and a counting frame of 50 × 50 μm were used for counting BrdU-positive cells in a grid size of 100 × 100 μm using the fractionator probe. The starting point of all the series was random. Data obtained with stereological methods were used to normalize the data obtained with confocal microscopy to the whole DG using arithmetical proportion.

Results

Tis21-GFP Is Specifically Expressed in the Neurogenic Regions of the Postnatal, Juvenile, and Adult Brain

We analyzed early postnatal (1 and 2 weeks postnatal—P1W and P2W), juvenile (P3W and P6W), young-adult (P9W), and adult (P18W and P36W) mice for *Tis21*-GFP fluorescence. *Tis21*-GFP was found in the neurogenic regions of the postnatal, juvenile, and adult brains (Fig. 1*A*). These regions are the SGZ in the hippocampus (Fig. 1*B*,*B*′, open triangles) and the subventricular zone (SVZ) of the forebrain (Fig. 1*C*,*C*′). We also found expression in the rostral migratory stream and in the granular cell layer of the olfactory bulb (OB) (Fig. 1*D*,*D*′, Supplementary Fig. 1*A*–*F*). In addition, *Tis21*-GFP–positive cells were found in the external GCL of the P1W cerebellum (Fig. 1*E*), where neurogenesis occurs for a limited period after birth. In addition and unexpectedly, a great number of *Tis21*-GFP–positive cells were found in the GCL of the DG itself (Fig. 1*B*,*B*′). In contrast, no *Tis21*-GFP–positive cells were found in the cerebral cortex or in other nonneurogenic regions of the adult brain. For the remainder of the study, we focused our analysis on the hippocampus (SGZ and GCL).

Tis21-GFP Is Expressed in both Proliferating Precursor Cells and Postmitotic Granule Cells

To investigate whether *Tis21*-GFP–positive cells are dividing precursor cells, we performed immunohistochemistry on the

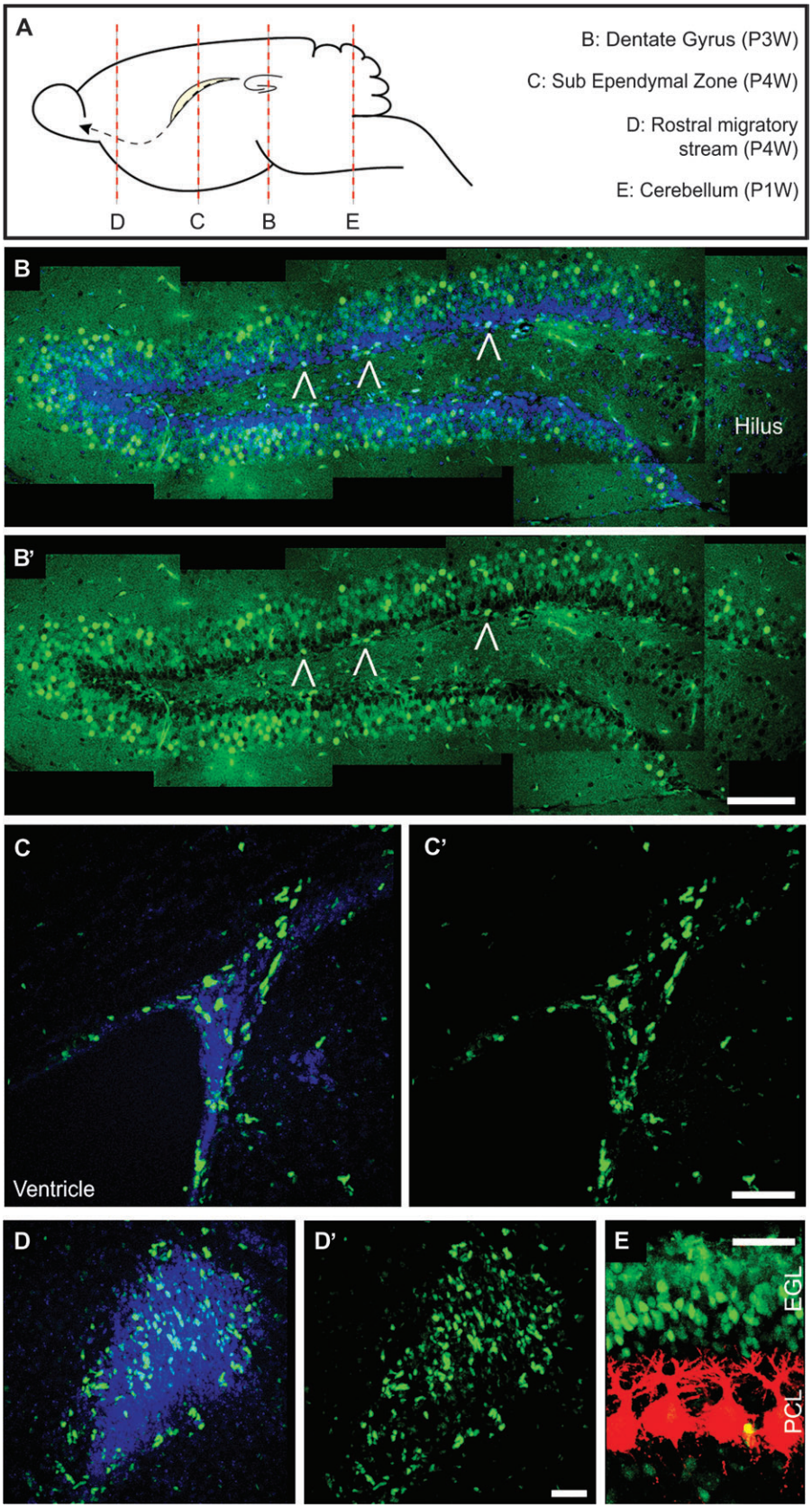

Figure 1. Intrinsic *Tis21*-GFP fluorescence in the postnatal and adult mouse brain. (*A*) Diagram showing the main postnatal neurogenic regions and indicating the position of the sections in (*B–E*). (*B–E*) Confocal scanning photomicrographs (single optical sections, 1 μm each) of 40-μm sections through the P3W DG (*B* and *B′*), P4W SVZ (*C–D′*), and P1W cerebellum (*E*) of *Tis21*-GFP mice showing intrinsic *Tis21*-GFP fluorescence (green) and CB (*E*, red) immunofluorescence; blue, Hoechst staining of nuclei (*B*, *C*, and *D*). (*B* and *B′*) are composite pictures including different optical fields. Open triangles indicate *Tis21*-GFP–positive cells in the SGZ. EGL, external GCL; PCL, Purkinje cell layer. Scale bars: (*B′*), 100 μm; (*C′*), 50 μm; (*D′*), 40 μm; (*E*), 30 μm.

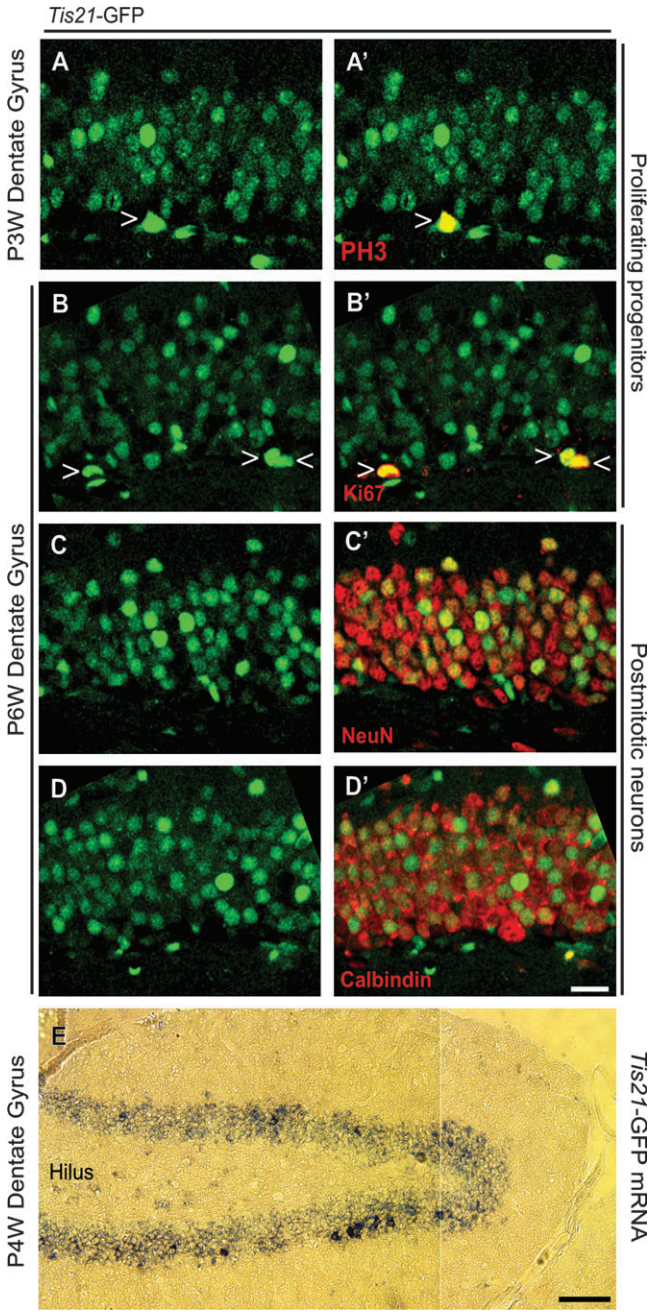

Figure 2. *Tis21*-GFP is expressed by mitotic progenitor cells as well as postmitotic granule cells. (*A–D′*) Confocal scanning photomicrographs (single optical sections, 1 μm each) of 40-μm sections through the P3W (*A* and *A′*) and P6W (*B–D′*) DG of *Tis21*-GFP mice showing intrinsic *Tis21*-GFP fluorescence (green) and its colocalization with PH3 (*A′* red, open triangle), Ki67 (*B′* red, open triangles), NeuN (*C′* red), and CB (*D′* red) immunofluorescence. (*E*) Bright-field photomicrograph of 10-μm cryosection through the P4W DG of *Tis21*-GFP mice showing in situ hybridization for *Tis21*-GFP mRNA (blue). The images in (*A–D′*) are oriented with the hilus at the bottom. Scale bars: (*D′*), 20 μm; (*E*), 100 μm.

P3W and P6W DG using antibodies against PH3 and Ki67. Of all PH3-positive mitotic cells detected in the SGZ, 50% were *Tis21*-GFP positive (e.g., see Fig. 2*A*,*A′*, open triangle). Of all Ki67-positive cells, 22% were *Tis21*-GFP positive (e.g., see Fig. 2*B*,*B′*, open triangles). These results show that a subset of *Tis21*-GFP–positive cells in the SGZ undergo cell cycle progression and mitosis.

During embryonic development, postmitotic neurons do not express Tis21 or *Tis21*-GFP but show GFP fluorescence for a short period after their birth because they passively inherit the protein from their progenitor (Iacopetti et al. 1999; Haubensak et al. 2004). Consequently, *Tis21*-GFP–expressing cells are essentially restricted to the germinal zones of the neuroepithelium (ventricular zone and SVZ) (Iacopetti et al. 1999; Haubensak et al. 2004). As we had here found a large number of *Tis21*-GFP–positive cells within the GCL, where no precursor cells are found, we next studied whether, in contrast to the situation in the fetal brain, *Tis21*-GFP is also expressed by postmitotic neurons in the neurogenic zone of the adult hippocampus.

Indeed, we observed that *Tis21*-GFP extensively colocalized with the neuronal marker NeuN and the granule cell marker CB (Fig. 2*C–D′*) (Celio et al. 1990; Mullen et al. 1992). We next investigated whether the *Tis21*-GFP fluorescence detected in DG neurons was caused by inheritance of the GFP from the progenitor or reflected de novo expression. In situ hybridization revealed that *Tis21*-GFP mRNA expression covered the entire width of the DG and was thus also found in cell layers of the DG, in which postmitotic neurons are located (Fig. 2*E*) (Kempermann et al. 2003). These results suggest that some granule cells transcribe *Tis21*-GFP, in contrast to embryonic development, where *Tis21* mRNA is not found in neurons (Iacopetti et al. 1999). Similar results were obtained in the OB where in situ hybridization revealed *Tis21*-GFP mRNA expression in the mature neurons (Supplementary Fig. 1*G*,*H*). The observed expression pattern of *Tis21*-GFP was consistent with the Tis21 (BTG2) expression data in the Allen Brain Atlas (http://www.brain-map.org) (Lein et al. 2007).

Abundance of Tis21-GFP–Positive Cells in the Postnatal and Mature DG

As we had found *Tis21*-GFP to be expressed in both precursor cells and granule cells of young animals, we next asked whether the abundance of *Tis21*-GFP–positive cells would change along with the change in the proportion of precursor cells versus neurons between early postnatal and adult time points.

During fetal brain development, the DG develops from precursor cells migrating from the hippocampal hem of the dorsal SVZ into the region that will become the hippocampus. Migration occurs in 2 waves: the first germinal matrix forms between 1 and 2 days before birth and the second germinal matrix follows between 2 and 3 days after birth. Precursor cells of the first and second germinal matrix give rise to the bulk of granule cells. Within the first weeks after birth, a third germinal matrix forms in the SGZ (Schlessinger et al. 1975; Rickmann et al. 1987; Altman and Bayer 1990a, 1990b).

We quantified the number of *Tis21*-GFP–positive cells in the entire DG at ages reflecting 1) the first and second germinal matrices (P1W and P2W; Fig. 3*A–B′*), 2) the onset of formation of the DG (P3W; Fig. 3*C–C′*), and 3) its maturity (P6W, P9W, and P18W; Fig. 3*D–F′*) when cell proliferation has become restricted to the third germinal matrix.

Although the number of *Tis21*-GFP–positive cells was variable between different animals of the same age, significant changes could be found between the age groups. The number of *Tis21*-GFP–positive cells first increased ($P < 0.001$) from P1W to P2W and then decreased from P2W to P3W ($P < 0.01$). From P3W to P9W, no significant difference was evident between the groups. Finally, the number of *Tis21*-GFP–positive cells

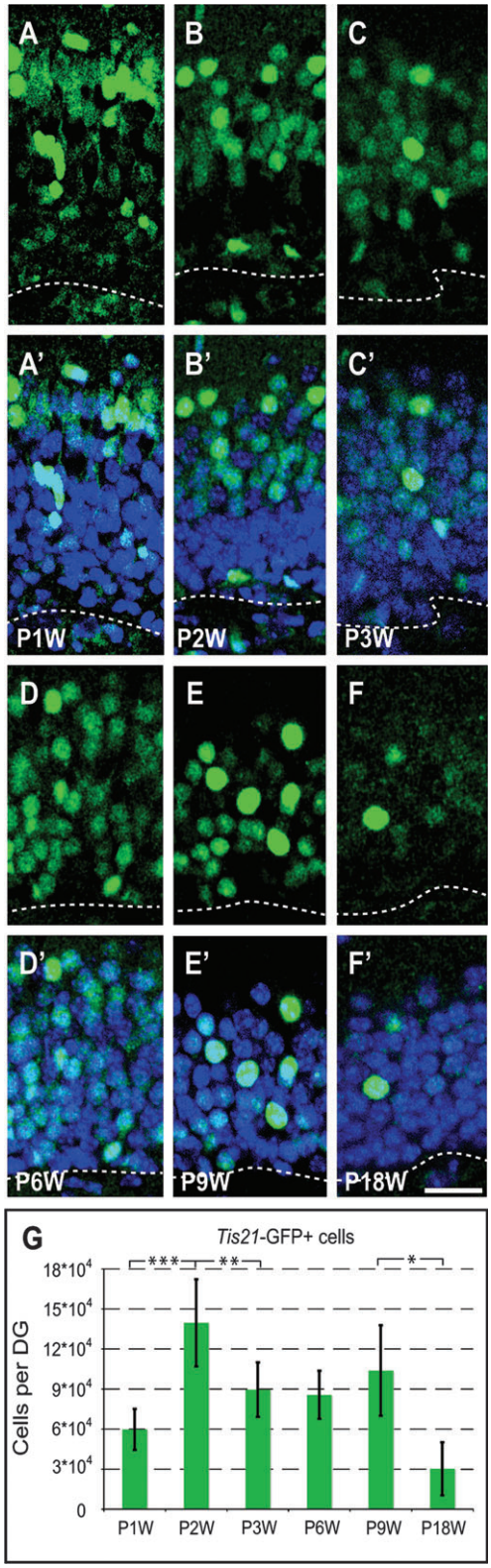

Figure 3. *Tis21*-GFP–positive cells during formation and maturation of the DG. (*A–F′*) Confocal scanning photomicrographs (single optical sections, 1 μm each) of 40-μm sections through the P1W (*A* and *A′*), P2W (*B* and *B′*), P3W(*C* and *C′*), P6W (*D* and *D′*), P9W (*E* and *E′*), and P18W (*F* and *F′*) DG of *Tis21*-GFP mice showing intrinsic *Tis21*-GFP fluorescence (green); blue, Hoechst staining of nuclei. Dashed lines, boundary to the hilus. Scale bar: (*F′*), 20 μm. (*G*) *Tis21*-GFP–positive cells (intrinsic fluorescence) per entire DG at various time points of postnatal development. Data are the mean of 3–12 animals; error bars indicate standard deviations. Triple asterisk, $P < 0.001$; double asterisk, $P < 0.01$; single asterisk, $P < 0.02$.

decreased ($P < 0.02$) from P9W to P18W. At the age of 36 weeks (P36W), the animals showed only very low *Tis21*-GFP fluorescence in the GCL (Supplementary Fig. 2*A–D*). These data indicate that the number of *Tis21*-GFP–positive cells is low during early phases of the formation of the DG when the majority of the cells in the future DG are proliferating precursor cells from the first and second germinal matrices. The number of *Tis21*-GFP–positive cells increases at the time when the postmitotic granule cells start to build up the GCL. After a significant decrease (P3W), *Tis21*-GFP expression remains relatively constant until young-adulthood (P9W), to further decrease to very low levels during maturity (P18W and P36W).

Characterization of Tis21-GFP–Expressing Precursor Cells

Given that *Tis21*-GFP is expressed in precursor cells of the SGZ and neurons of the GCL, we sought to determine whether *Tis21*-GFP expression was restricted to only certain stages of adult hippocampal neurogenesis.

To investigate this issue during early ages and maturity, we quantified the overlap between the *Tis21*-GFP expression and immunoreactivity for markers of the different stages of neuronal development in the adult DG (Kempermann et al. 2004; Steiner et al. 2006).

To assess *Tis21*-GFP expression in radial glia–like stem cells (type-1) and astrocytes, we used antibodies against GFAP, S100β, and nestin. We could not detect cells double positive for *Tis21*-GFP and GFAP, S100β, or nestin, suggesting that cells with these radial glia–like or astrocytic features did not express *Tis21*-GFP (Supplementary Fig. 2*E–G*).

To identify precursor cells with nonradial morphology that were not yet restricted to a neuronal fate (type-2a), we used Sox2 and Blbp as markers (Feng et al. 1994; D'Amour and Gage 2003; Komitova and Eriksson 2004; Steiner et al. 2006; Jessberger et al. 2008). We found Sox2- and Blbp/*Tis21*-GFP–double-positive cells in the SGZ (Fig. 4*A*, open triangles; Supplementary Fig. 2*H*, open triangles), indicative of *Tis21*-GFP in type-2a cells and also in the SVZ (Supplementary Fig. 1*A*, open triangles). The number of Sox2/*Tis21*-GFP–double-positive cells decreased concomitant with the overall decrease of the Sox2 cell population (Fig. 4*A′*; see also Supplementary Table 1).

To identify lineage-determined progenitor cells (type-2b and 3), we studied expression of Dcx and NeuroD1 (Seki 2002; Brown et al. 2003; Rao and Shetty 2004; Couillard-Despres et al. 2005). In the DG, Dcx is found in dividing neuronal precursor cells (around 20% of the all Dcx-positive cells represent type-2b and 3 cells) as well as in immature neurons (around 70% of the all Dcx-positive cells are postmitotic) (Plumpe et al. 2006). Moreover, Dcx is expressed after Sox2, and both markers show very little overlap (Steiner et al. 2006). As with Sox2, we found double-positive Dcx- and NeuroD1/*Tis21*-GFP cells in the SGZ (Fig. 4*B*, open triangles; Supplementary Fig. 2*I*, open triangle). However, in both the SVZ and OB, there was hardly any colocalization between *Tis21*-GFP and Dcx (Supplementary Fig. 1*B,D*). The number of Dcx/*Tis21*-GFP–double-positive cells decreased with the reduction of the Dcx cell population, thus showing a pattern similar to the Sox2/*Tis21*-GFP–double-positive cell population (Fig. 4*B′*; see also Supplementary Table 1).

Taken together, these data suggest that during postnatal and adult neurogenesis in the DG, Tis21 is not expressed in the

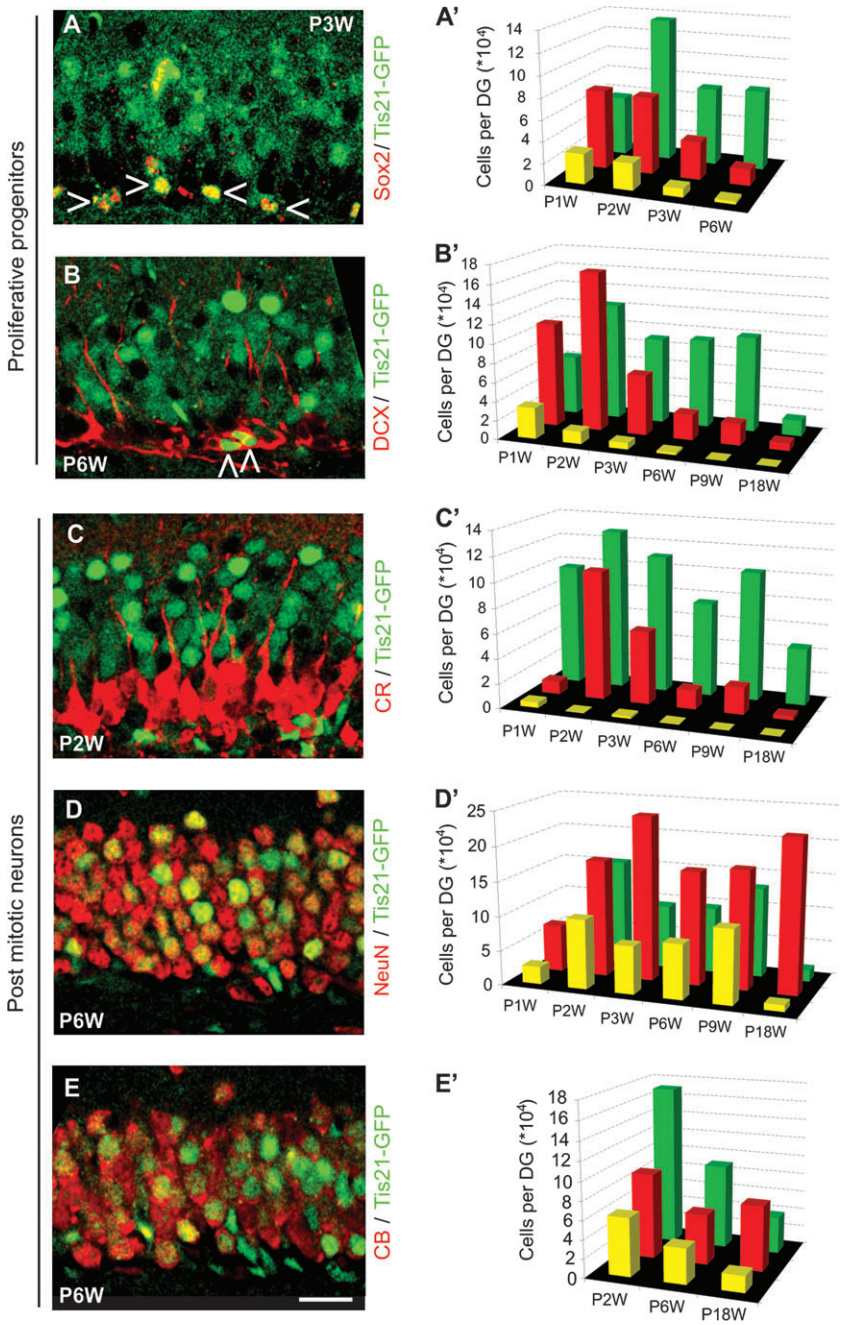

Figure 4. *Tis21*-GFP expression in precursor cells and postmitotic neurons during formation and maturation of the DG. (*A*–*E*) Confocal scanning photomicrographs (single optical sections, 1 μm each) of 40-μm sections through the P3W (*A*), P6W (*B*, *D*, *E*), and P2W (*C*) DG of *Tis21*-GFP mice showing intrinsic *Tis21*-GFP fluorescence (green) and Sox2 (*A*), Dcx (*B*), CR (*C*), NeuN (*D*), and CB (*E*) immunofluorescence (red). Open triangles indicate *Tis21*-GFP–positive cells that are immunoreactive for Sox2 (*A*) or Dcx (*B*). Scale bar: (*E*), 20 μm. (*A′*–*E′*) Green bars indicate the number of *Tis21*-GFP–positive cells; red bars the number of Sox2- (*A′*), Dcx- (*B′*), CR- (*C′*), NeuN- (*D′*), and CB (*E′*)-positive cells and yellow bars the number of cells double positive for *Tis21*-GFP and the respective marker, in each case per entire DG. Data are the mean of 2–10 animals; here no error bars are shown for clarity.

radial glia–like stem cell population but is expressed, in particular at the early postnatal stage, in Sox2-, Blbp-, Dcx-, and NeuroD1-positive precursor cells. This indicates Tis21 expression from type-2a cells onward.

Characterization of the Tis21-GFP–Expressing Postmitotic Cells

To characterize *Tis21*-GFP expression at later stages of adult hippocampal neurogenesis, we used CR, a calcium-binding protein that, in the DG, is expressed in early postmitotic immature granule cells and shows overlapping expression with Dcx (Brandt et al. 2003). Remarkably, we found very few CR/*Tis21*-GFP–double-positive cells at P1W and hardly any thereafter (Fig. 4*C*,*C′*; see also Supplementary Table 1). Relatedly, very few double-positive cells could be found in the OB of 6-week-old animals (Supplementary Fig. 1*E*).

We completed our time course analysis by determining the abundance of *Tis*-GFP–positive cells among mature granule

cells expressing NeuN or CB. Double-positive cells were found at all time points between P1W and P18W (Fig. 4*D*,*E*). Only some NeuN- or CB-positive neurons were *Tis21*-GFP positive, and the total number of NeuN/*Tis21*-GFP–double-positive cells decreased at P18W (Supplementary Table 1). As in the DG, *Tis21*-GFP/NeuN-positve cells were also found in the OB (Supplementary Fig. 1*F*, open triangles).

Tis21-GFP Expression Marks Both Populations of Neurogenic Precursor Cells and New Postmitotic Neurons

The data presented so far provided information on the abundance of *Tis21*-GFP–positive cells in the postnatal and adult DG, their status in respect to the cell cycle (PH3 and Ki67), and the overlap with various markers commonly used to define specific stages of adult neurogenesis. To obtain more direct evidence for the lineage relationship of the *Tis21*-GFP–positive cells, we combined the above-described analyses with a BrdU pulse-chase experiment. Specifically, we labeled precursors at P3W by 2 consecutive injections with BrdU (3-h interval) and analyzed their progeny at various time points thereafter (24 h, 3 days, 1, 2, 4, 6, and 9 weeks after injection; Fig. 5*A*). At each time point, we studied 1) the total number of BrdU-positive cells per DG (Fig. 5*D*, red curve), 2) the number of *Tis21*-GFP–positive cells in the BrdU-positive cell population (Fig. 5*D*, green bars; Fig. 5*F*, green curve), and 3) how many of these cells additionally expressed selected markers (Fig. 5*E*–*F*).

The total number of BrdU-positive cells changed over time after injection in agreement with the known dynamic pattern (Kempermann et al. 2004). The numbers declined within the first 2 weeks after BrdU administration and remained relatively stable thereafter (Fig. 5*D*, red curve). Initially (24 h after BrdU injection), 31.9 ± 1.3% of the BrdU-positive cells were *Tis21*-GFP positive (Fig. 5*D*, green bars). A portion of these BrdU/*Tis21*-GFP–double-positive cells was immunoreactive for Sox2 (36%) and Dcx (13%), whereas expression of the neuronal markers was barely detectable (Fig. 5*E*). Remarkably, whereas the number of BrdU-labeled cells and the proportion of BrdU/*Tis21*-GFP–double-positive cells were very similar at 3 days (29.2 ± 4.6%) compared with 24 h after the BrdU injections (Fig. 5*D*), the number of cells triple positive for BrdU/*Tis21*-GFP plus either Sox2 or Dcx was lower by a quarter (9% and 4%, respectively) from 24 h to 3 days postinjection (p.i.), without a corresponding appearance of cells triple positive for BrdU/*Tis21*-GFP plus a neuronal marker (Fig. 5*E*). This decrease was paralleled by a similar decrease with respect to Sox2 versus Dcx.

At 1 week after BrdU injection, the total number of BrdU-labeled cells had decreased by more than half (Fig. 5*D*, red curve) and that of the BrdU/*Tis21*-GFP–double-positive cells had dropped even more (6% as compared with 3 days p.i.; Fig. 5*D*, green bars). The number of BrdU/*Tis21*-GFP–double-positive cells remained at that low level for another 3 weeks and then increased (Fig. 5*F*), constituting 10% (at P2W) to almost 80% (at P9W) of all BrdU-labeled cells (Fig. 5*D*). Concomitant with this, an increasing proportion of the BrdU/*Tis21*-GFP–double-positive cells expressed markers of postmitotic neurons, that is, NeuN and CB (Fig. 5*E*–*F*).

Discussion

In the postnatal and adult mouse brain, *Tis21*-GFP expression is restricted to those regions where neurogenesis continues to occur. By focusing on the DG and comparing the expression of *Tis21*-GFP with various markers previously used to define the precursor lineage and granule cell maturation (Kempermann et al. 2004; Steiner et al. 2006), our study contributes 2 novel findings: 1) the identification of a *Tis21*-GFP–positive progenitor subpopulation that lacks canonical progenitor markers and 2) the demonstration of *Tis21*-GFP expression in postmitotic neurons.

A Tis21-GFP–Positive Progenitor Subpopulation Lacking Canonical Progenitor Markers

With regard to the various subpopulations of precursor cells (Fig. 6), our classification into type-1, 2a/b, and 3 cells was initially based on the expression of nestin-GFP and Dcx, proliferative activity, as well as morphological criteria. The scheme corresponds to the sequence of "radial glia–like precursor cell," "glia-like transient amplifying progenitor cell," "neuronally determined transient amplifying progenitor cell," and "migratory neuroblast" (Kempermann et al. 2004; Steiner et al. 2006, 2008). The equivalence between these 2 terminologies is largely inferred, however, and still subject to discussion. We have used the expression of Sox2, Blbp, Prox1, and NeuroD1 as additional markers to describe the initial developmental stages in the course of adult neurogenesis (Steiner et al. 2006, 2008). Others have introduced markers such as HOP (De Toni et al. 2008), Tbr2 (Hodge et al. 2008), and Ascl1 (Kim et al. 2007). Although these additional markers have in general confirmed the above classification, it is likely that the current operational nomenclature will be subject to future refinement. To facilitate the discussion here, we have projected our present data obtained for Tis21 onto the original model, which had been based on *Nestin*-GFP and Dcx, as have done by others (Breunig et al. 2007; von Bohlen und Halbach 2007).

Considering these limitations of the present classification, we did not detect *Tis21*-GFP expression in cells with radial morphology positive for nestin, GFAP, or S-100 beta, that is, the type-1 radial glia–like stem cells. *Tis21*-GFP expression was first detected in nonradial type-2a progenitor cells expressing Sox2 and Blbp. Using BrdU pulse-chase analysis, the first cell subpopulation in which *Tis21*-GFP expression was detected were Sox2- and Dcx-positive cells (Fig. 5*E*).

Importantly, the number of BrdU/*Tis21*-GFP–double-positive cells remained constant between 24 h and 3 days after BrdU injection but dropped dramatically thereafter (Fig. 5*D*). This drop presumably reflected dilution of the BrdU label due to multiple rounds of cell division (see below), which implies that most, if not all, of the BrdU/*Tis21*-GFP–double-positive cells observed at 24 h and 3 days after injection were precursor cells. In addition, the parallel decrease from 24 h to 3 days in the proportion of BrdU/*Tis21*-GFP–double-positive cells showing Sox2 and Dcx immunoreactivity (Fig. 5*E*) implies that the vast majority (>85%) of the BrdU/*Tis21*-GFP–double-positive cells at 3 days lack Sox2 and Dcx expression. We propose that these Sox2- and Dcx-negative and *Tis21*-GFP–positive cells represent a neuronally committed progenitor subpopulation from which granule cells originate during postnatal and adult neurogenesis in the DG.

Heterogeneity of subpopulations of hippocampal precursor cells has been suggested for other factors, for example, proneural basic helix-loop-helix transcription factor Neurogenin2 (Ngn2). Ngn2 (Raineteau et al. 2006; Ozen et al. 2007). In this context, Ngn2 is especially interesting because its

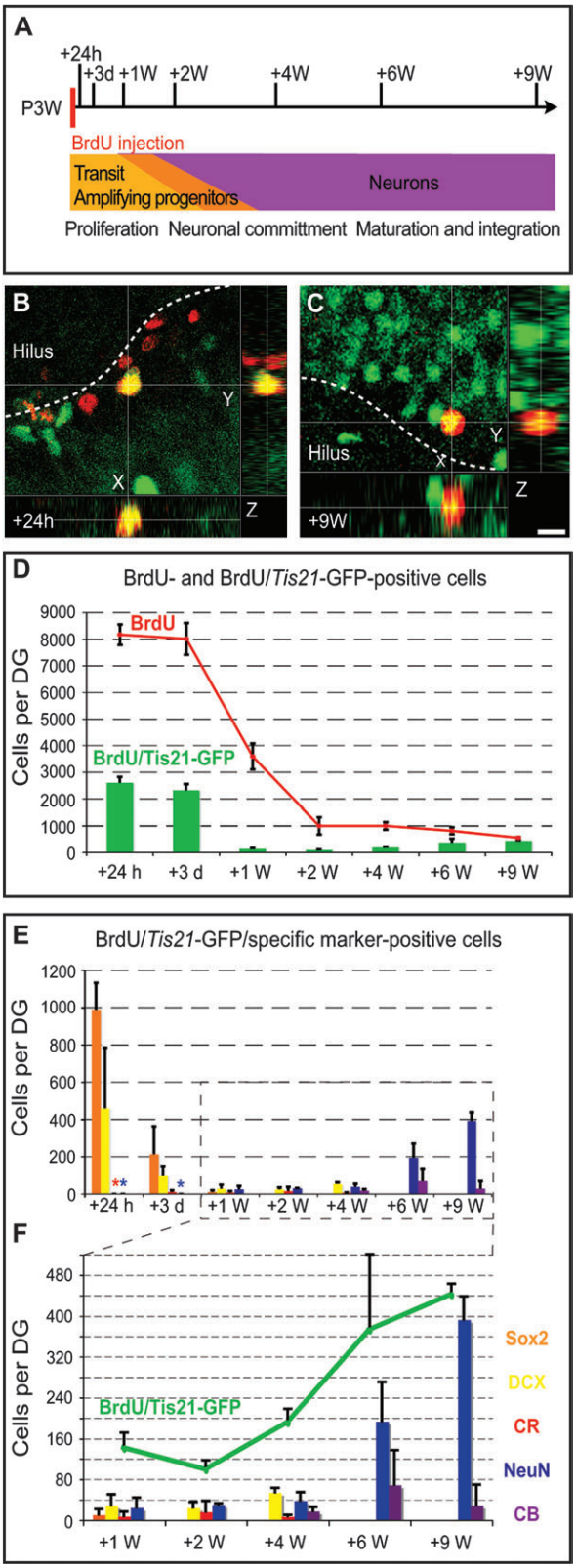

Figure 5. BrdU pulse chase for *Tis21*-GFP cells. (*A*) Schematic drawing showing the pulse-chase strategy in relation to postnatal DG development: 3-week-old *Tis21*-GFP heterozygous mice were injected with BrdU (50 mg/kg) twice, with a 3-h interval between injections. Brains were collected 24 h, 3 days, and 1, 2, 4, 6, and 9 weeks after injection. (*B–C*) Confocal scanning photomicrographs and stacks of 7 (*B*) and 6 (*C*) single optical sections (1 μm each) of 40-μm-thick sections through the P3W + 24 h (*B*) and P3W + 9 weeks (*C*) DG of *Tis21*-GFP mice showing *Tis21*-GFP (green) and BrdU (red) double immunofluorescence. Dashed lines, boundary to the hilus. Scale bar in (*C*), 10 μm. (*D*) Number of total BrdU-positive cells (red curve) and the BrdU-positive cells showing *Tis21*-GFP immunofluorescence (green bars) per entire DG at various time points after the BrdU pulse. Data are the mean of 3 animals; error bars indicate standard deviations. (*E–F*) Number of BrdU/*Tis21*-GFP–double-positive cells showing Sox2 (orange), Dcx (yellow), CR (red), NeuN (blue), and the CB (purple) immunoreactivity per entire DG at various time points after the BrdU pulse. Number of BrdU/*Tis21*-GFP–double-positive cells (green curve) compared with BrdU/*Tis21*-GFP–double-positive cells showing Sox2 (orange bars), Dcx (yellow bars), CR (red bars), NeuN (blue bars), and CB (purple bars) immunoreactivity per entire DG at selected time points after the BrdU pulse. Data are the mean of 2 or 3 animals; bars indicate standard deviation in all cases in which 3 animals were analyzed and standard error at P24h and P9W for CB where 2 animals were examined. Asterisks in the respective colors indicate that no positive cell could be detected (but the analysis was done).

expression pattern is consistent with either transient expression in amplifying precursor cells before cell cycle exit or the existence of 2 subpopulations (Ngn2 positive or negative) with different cell fates, as it might be the case for Tis21 as well.

Tis21-GFP Expression in Postmitotic Neurons

Following their drop after 3 days after injection, the number of BrdU/*Tis21*-GFP–double-positive cells gradually increased from 1 to 9 weeks p.i., and an increasing proportion of them expressed postmitotic marker NeuN (from 18% at 1 week to 89% at 9 weeks after injection; Fig. 5*D–F*). Thus, in contrast to the fetal brain, where postmitotic neurons do not express Tis21 (Iacopetti et al. 1994, 1999) and might show inherited *Tis21*-GFP fluorescence only immediately after their birth (Haubensak et al. 2004), in the postnatal and adult DG, Tis21 (as revealed by *Tis21*-GFP) is also expressed in postmitotic neurons.

Our conclusion that Tis21 is expressed in maturing postmitotic granule cells is supported by 2 additional lines of evidence. First, at P4W, when essentially all granule cells are still young and immature, we detected *Tis21*-GFP mRNA in the vast majority of granule cells (Fig. 2*E*). Second, a substantial proportion of NeuN- and CB-positive mature neurons was *Tis21*-GFP positive (Fig. 4). However, *Tis21*-GFP expression did not persist after granule cell maturation, as the proportion of NeuN- and CB-positive cells showing *Tis21*-GFP expression decreased by P18W (Fig. 4) and even more at P36W (Supplementary Fig. 2*B*).

Interestingly, a proportion of BrdU/*Tis21*-GFP–double-positive cells between 1 and 4 weeks after BrdU injection expressed Dcx and to a small extent CR and later from 4 to 9 weeks CB and NeuN (Fig. 5*F*). Moreover, during postnatal DG development and maturation, the number of *Tis21*-GFP–positive CB-expressing neurons was substantially greater than that of the CR-expressing neurons, which was very low (Fig. 4). These data are consistent with the following scenarios. Newborn immature neurons initially lack *Tis21*-GFP expression, which is only induced upon maturation of these neurons, when Dcx and CR are downregulated and CB is upregulated (Fig. 6). Alternatively, *Tis21*-GFP expression is maintained in newborn neurons which originate from *Tis21*-GFP–expressing progenitor cells and which express CB; by contrast, CR and Dcx expression marks a distinct subpopulation of immature neurons largely devoid of *Tis21*-GFP expression. Further work is required to resolve this issue.

Significance of Tis21-GFP Expression in Maturing Granule Cells

It is likely that Tis21 serves 2 distinct functions: one in neural precursor cells, which is shared between fetal and adult

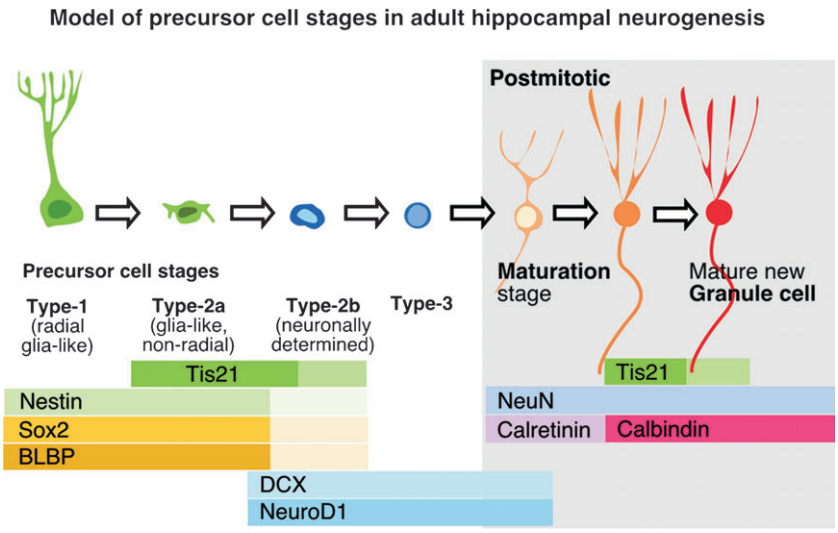

Figure 6. *Tis21*-GFP expression in the course of adult hippocampal neurogenesis. Simplified schematic drawing showing a model of adult hippocampal neurogenesis and *Tis21*-GFP expression in relation to expression of other markers along the cell lineage of the DG.

neurogenesis, and one that is specific for adult-generated granule cells in the course of their maturation. At present, we can only speculate about the nature of this second function.

Considering the inhibitory role of Tis21 in cell cycle progression known from embryonic and fetal neurogenesis (Canzoniere et al. 2004; Calegari et al. 2005), the postmitotic state of adult-generated granule cells might require consolidation by expression of antiproliferative factors such as Tis21. Consistent with this hypothesis, activation of Tis21 in hippocampal progenitor cells led to an accelerated transition from a proliferative precursor cell to a postmitotic maturing cell (Farioli-Vecchioli et al. 2008).

Alternatively, Tis21 expression in maturing granule cells might be linked to the fact that these cells, in contrast to embryonic neurogenesis, integrate into already existing neuronal networks and are subject to the inputs of various neurotransmitter systems during this process (Deisseroth et al. 2004; Ming and Song 2005; Tozuka et al. 2005; Plumpe et al. 2006). For example, Tis21 expression might be linked to the switch to full synaptic integration and glutamatergic innervation. The time window of 2–9 weeks, in which we observed *Tis21*-GFP reexpression, matches with the period, during which the newly generated granule cells exhibit increased synaptic plasticity, and are more likely to be incorporated in preexisting circuits (Schmidt-Hieber et al. 2004; Ge et al. 2007; Kee et al. 2007). From these observations, we might hypothesize that Tis21 reexpression in maturing neurons is related to the establishment of excitatory neurotransmission.

The Population of Tis21-GFP–Positive Cells Reflects the Waves of Neurogenesis in the Postnatal DG

The DG develops from progenitor cells migrating in from the hippocampal hem in 2 waves forming the first and the second germinal matrices (Altman and Bayer 1990a, 1990b). We propose that the variation of the number of *Tis21*-GFP–positive cells early postnatally and during adulthood reflects, at least in part, the remnants of these waves of granule cell production and thus, in general, mirrors the temporal changes in the rate of neurogenesis. The strong increase in the number of *Tis21*-GFP–positive cells between P1W and P2W (Fig. 3*G*) correlates with the first appearance of granule cells generated pre- and perinatally. The increase in the number of the *Tis21*-GFP–positive cells between P1W and P2W might reflect the switch from a stage in which the GCL is still mostly formed by progenitor cells (first and second germinal matrices, most of which are *Tis21*-GFP negative) to a stage at which the majority of cells in the region of the GCL have become granule cells (Fig. 4*B′*,*C′*,*D′*), which are then mostly *Tis21*-GFP positive.

When the second germinal matrix transforms into the much less active third germinal matrix, the rate of neurogenesis decreases significantly (as confirmed by the decrease of the number of Dcx- and CR-positive cells between P2W and P3W, Fig. 4*B′*,*C′*, as well the parallel decrease in cell proliferation). This event temporally correlates with a significant decrease in the number of *Tis21*-GFP–positive cells between P2W and P3W.

The same might hold true for the decrease in the number of *Tis21*-GFP–positive cells observed between P9W and P18W. Between P3W and P9W, the rate of neurogenesis would be in a stable equilibrium with *Tis21*-GFP degradation, so that the numbers of *Tis21*-GFP–positive cells were constant over this period. However, with increasing age, the rate of neurogenesis decreases, changing this equilibrium, ultimately leading to the decline in number of *Tis21*-GFP–positive cells that we observe between P9W and P18W.

In conclusion, the variation of the number of *Tis21*-GFP–positive cells in the GCL is likely to reflect the changes in the rate of adult hippocampal neurogenesis. In addition, because much of the selection on the newly generated granule cells occurs during early stages of maturation, the number of neuronal *Tis21*-GFP–positive cells might mirror the number of newly generated granule cells that reach maturity. With this, Tis21 might become an interesting target to study the late stages of adult hippocampal neurogenesis.

Supplementary Material

Supplementary material can be found at http://www.cercor.oxfordjournals.org/.

Funding

Stipend from International Max Planck Research School for Molecular Cell Biology and Bioengineering to AA; MeDDrive grants from the University of Dresden to KF and JK; Deutsche Forschungsgemeinschaft (DFG) Research Center for Regenerative Therapies Dresden, funded by the Deutsche Forschungsgemeinschaft to GK; Deutsche Forschungsgemeinschaft (SPP 1109, Hu 275/7-3; SPP 1111, Hu 275/8-3; SFB/TR 13, B1; SFB 655, A2); Fonds der Chemischen Industrie; Federal Ministry of Education and Research (BMBF) in the framework of the National Genome Research Network (NGFN-2) to WBH.

Notes

We thank the facilities of MPI-CBG, especially J. Helppi and the mouse facility, for excellent support. In addition, the generous support of the neurobiology laboratory in the Department of Psychiatry is gratefully acknowledged. We thank Dr Federico Calegari for his helpful comments on the manuscript and Ji Feng Fei for his help with in situ hybridization. AA was a member of the International Max Planck Research School for Molecular Cell Biology and Bioengineering; JK was a member of the International Max Planck Research School "Life Course: Evolutionary and Ontogenetic Dynamics" (LIFE). WBH and GK are the joint senior authors. *Conflict of Interest*: None declared.

Address correspondence to email: gerd.kempermann@crt.dresden.de.

References

Altman J, Bayer SA. 1990a. Migration and distribution of two populations of hippocampal granule cell precursors during the perinatal and postnatal periods. J Comp Neurol. 301:365–381.

Altman J, Bayer SA. 1990b. Vertical compartmentation and cellular transformations in the germinal matrices of the embryonic rat cerebral cortex. Exp Neurol. 107:23–35.

Attardo A, Calegari F, Haubensak W, Wilsch-Brauninger M, Huttner WB. 2008. Live imaging at the onset of cortical neurogenesis reveals differential appearance of the neuronal phenotype in apical versus basal progenitor progeny. PLoS ONE. 3:e2388.

Brandt MD, Jessberger S, Steiner B, Kronenberg G, Reuter K, Bick-Sander A, von der Behrens W, Kempermann G. 2003. Transient calretinin expression defines early postmitotic step of neuronal differentiation in adult hippocampal neurogenesis of mice. Mol Cell Neurosci. 24:603–613.

Breunig JJ, Silbereis J, Vaccarino FM, Sestan N, Rakic P. 2007 Dec 18. Notch regulates cell fate and dendrite morphology of newborn neurons in the postnatal dentate gyrus. Proc Natl Acad Sci USA. 104(51):20558–20563.

Brown JP, Couillard-Despres S, Cooper-Kuhn CM, Winkler J, Aigner L, Kuhn HG. 2003. Transient expression of doublecortin during adult neurogenesis. J Comp Neurol. 467:1–10.

Calegari F, Haubensak W, Haffner C, Huttner WB. 2005. Selective lengthening of the cell cycle in the neurogenic subpopulation of neural progenitor cells during mouse brain development. J Neurosci. 25:6533–6538.

Canzoniere D, Farioli-Vecchioli S, Conti F, Ciotti MT, Tata AM, Augusti-Tocco G, Mattei E, Lakshmana MK, Krizhanovsky V, Reeves SA, et al. 2004. Dual control of neurogenesis by PC3 through cell cycle inhibition and induction of Math1. J Neurosci. 24:3355–3369.

Celio MR, Baier W, Scharer L, Gregersen HJ, de Viragh PA, Norman AW. 1990. Monoclonal antibodies directed against the calcium binding protein calbindin D-28k. Cell Calcium. 11:599–602.

Couillard-Despres S, Winner B, Schaubeck S, Aigner R, Vroemen M, Weidner N, Bogdahn U, Winkler J, Kuhn HG, Aigner L. 2005. Doublecortin expression levels in adult brain reflect neurogenesis. Eur J Neurosci. 21:1–14.

D'Amour KA, Gage FH. 2003. Genetic and functional differences between multipotent neural and pluripotent embryonic stem cells. Proc Natl Acad Sci USA. 100(Suppl 1):11866–11872.

Deisseroth K, Singla S, Toda H, Monje M, Palmer TD, Malenka RC. 2004. Excitation-neurogenesis coupling in adult neural stem/progenitor cells. Neuron. 42:535–552.

De Toni A, Zbinden M, Epstein JA, Ruiz i Altaba A, Prochiantz A, Caillé I. 2008 May 28. Regulation of survival in adult hippocampal and glioblastoma stem cell lineages by the homeodomain-only protein HOP. Neural Dev. 3:13.

Farioli-Vecchioli S, Saraulli D, Costanzi M, Pacioni S, Cina I, Aceti M, Micheli L, Bacci A, Cestari V, Tirone F. 2008. The timing of differentiation of adult hippocampal neurons is crucial for spatial memory. PLoS Biol. 6:e246.

Feng L, Hatten ME, Heintz N. 1994. Brain lipid-binding protein (BLBP): a novel signaling system in the developing mammalian CNS. Neuron. 12:895–908.

Ge S, Yang CH, Hsu KS, Ming GL, Song H. 2007. A critical period for enhanced synaptic plasticity in newly generated neurons of the adult brain. Neuron. 54:559–566.

Guardavaccaro D, Corrente G, Covone F, Micheli L, D'Agnano I, Starace G, Caruso M, Tirone F. 2000. Arrest of G(1)-S progression by the p53-inducible gene PC3 is Rb dependent and relies on the inhibition of cyclin D1 transcription. Mol Cell Biol. 20:1797–1815.

Haubensak W, Attardo A, Denk W, Huttner WB. 2004. Neurons arise in the basal neuroepithelium of the early mammalian telencephalon: a major site of neurogenesis. Proc Natl Acad Sci USA. 101: 3196–3201.

Hodge RD, Kowalczyk TD, Wolf SA, Encinas JM, Rippey C, Enikolopov G, Kempermann G, Hevner RF. 2008 Apr 2. Intermediate progenitors in adult hippocampal neurogenesis: Tbr2 expression and coordinate regulation of neuronal output. J Neurosci. 28(14):3707–3717.

Iacopetti P, Barsacchi G, Tirone F, Maffei L, Cremisi F. 1994. Developmental expression of PC3 gene is correlated with neuronal cell birthday. Mech Dev. 47:127–137.

Iacopetti P, Michelini M, Stuckmann I, Oback B, Aaku-Saraste E, Huttner WB. 1999. Expression of the antiproliferative gene TIS21 at the onset of neurogenesis identifies single neuroepithelial cells that switch from proliferative to neuron-generating division. Proc Natl Acad Sci USA. 96:4639–4644.

Jessberger S, Toni N, Clemenson GD, Jr, Ray J, Gage FH. 2008. Directed differentiation of hippocampal stem/progenitor cells in the adult brain. Nat Neurosci. 11:888–893.

Kee N, Teixeira CM, Wang AH, Frankland PW. 2007. Preferential incorporation of adult-generated granule cells into spatial memory networks in the dentate gyrus. Nat Neurosci. 10:355–362.

Kempermann G, Gast D, Kronenberg G, Yamaguchi M, Gage FH. 2003. Early determination and long-term persistence of adult-generated new neurons in the hippocampus of mice. Development. 130(2): 391–399.

Kempermann G, Jessberger S. 2003. Adult-born hippocampal neurons mature into activity dependent responsiveness. Eur J Neurosci. 18(10):2707–2712.

Kempermann G, Jessberger S, Steiner B, Kronenberg G. 2004. Milestones of neuronal development in the adult hippocampus. Trends Neurosci. 27:447–452.

Kim EJ, Leung CT, Reed RR, Johnson JE. 2007 Nov 21. In vivo analysis of Ascl1 defined progenitors reveals distinct developmental dynamics during adult neurogenesis and gliogenesis. J Neurosci. 27(47): 12764–12774.

Komitova M, Eriksson PS. 2004. Sox-2 is expressed by neural progenitors and astroglia in the adult rat brain. Neurosci Lett. 369: 24–27.

Lein ES, Hawrylycz MJ, Ao N, Ayres M, Bensinger A, Bernard A, Boe AF, Boguski MS, Brockway KS, Byrnes EJ, et al. 2007. Genome-wide atlas of gene expression in the adult mouse brain. Nature. 445:168–176.

Ming GL, Song H. 2005. Adult neurogenesis in the mammalian central nervous system. Annu Rev Neurosci. 28:223–250.

Mullen RJ, Buck CR, Smith AM. 1992. NeuN, a neuronal specific nuclear protein in vertebrates. Development. 116:201–211.

Ozen I, Galichet C, Watts C, Parras C, Guillemot F, Raineteau O. 2007. Proliferating neuronal progenitors in the postnatal hippocampus transiently express the proneural gene Ngn2. Eur J Neurosci. 25: 2591–2603.

Plumpe T, Ehninger D, Steiner B, Klempin F, Jessberger S, Brandt M, Romer B, Rodriguez GR, Kronenberg G, Kempermann G. 2006. Variability of doublecortin-associated dendrite maturation in adult hippocampal neurogenesis is independent of the regulation of precursor cell proliferation. BMC Neurosci. 7:77.

Raineteau O, Hugel S, Ozen I, Rietschin L, Sigrist M, Arber S, Gahwiler BH. 2006. Conditional labeling of newborn granule cells to visualize their integration into established circuits in hippocampal slice cultures. Mol Cell Neurosci. 32:344–355.

Rao MS, Shetty AK. 2004. Efficacy of doublecortin as a marker to analyse the absolute number and dendritic growth of newly generated neurons in the adult dentate gyrus. Eur J Neurosci. 19:234–246.

Rickmann M, Amaral DG, Cowan WM. 1987. Organization of radial glial cells during the development of the rat dentate gyrus. J Comp Neurol. 264:449–479.

Rouault JP, Falette N, Guehenneux F, Guillot C, Rimokh R, Wang Q, Berthet C, Moyret-Lalle C, Savatier P, Pain B, et al. 1996. Identification of BTG2, an antiproliferative p53-dependent component of the DNA damage cellular response pathway. Nat Genet. 14:482–486.

Schlessinger AR, Cowan WM, Gottlieb DI. 1975. An autoradiographic study of the time of origin and the pattern of granule cell migration in the dentate gyrus of the rat. J Comp Neurol. 159:149–175.

Schmidt-Hieber C, Jonas P, Bischofberger J. 2004. Enhanced synaptic plasticity in newly generated granule cells of the adult hippocampus. Nature. 429:184–187.

Seki T. 2002. Expression patterns of immature neuronal markers PSA-NCAM, CRMP-4 and NeuroD in the hippocampus of young adult and aged rodents. J Neurosci Res. 70:327–334.

Song H, Kempermann G, Overstreet Wadiche L, Zhao C, Schinder AF, Bischofsberger J. 2005. New neurons in the adult mammalian brain: synaptogenesis and functional integration. J Neurosci. 25(45): 10366–10368.

Steiner B, Klempin F, Wang L, Kott M, Kettenmann H, Kempermann G. 2006. Type-2 cells as link between glial and neuronal lineage in adult hippocampal neurogenesis. Glia. 54: 805–814.

Steiner B, Zurborg S, Hörster H, Fabel K, Kempermann G. 2008 Jun 23. Differential 24 h responsiveness of Prox1-expressing precursor cells in adult hippocampal neurogenesis to physical activity, environmental enrichment, and kainic acid-induced seizures. Neuroscience. 154(2):521–529.

Tozuka Y, Fukuda S, Namba T, Seki T, Hisatsune T. 2005. GABAergic excitation promotes neuronal differentiation in adult hippocampal progenitor cells. Neuron. 47:803–815.

van Praag H, Schinder AF, Christie BR, Toni N, Palmer TD, Gage FH. 2002. Functional neurogenesis in the adult hippocampus. Nature. 415:1030–1034.

von Bohlen und Halbach O. 2007. Immunohistological markers for staging neurogenesis in adult hippocampus. Cell Tissue Res. 329:409–420.